

High-accuracy coherent optical frequency transfer over a doubled 642-km fiber link

Original

High-accuracy coherent optical frequency transfer over a doubled 642-km fiber link / D., Calonico; C., Calosso; Clivati, Cecilia; Costanzo, Giovanni Antonio; A., Godone; M., Frittelli; A., Mura; N., Poli; D. V., Sutyryn; G. M., Tino; M., Zucco; F., Levi. - In: APPLIED PHYSICS. B, LASERS AND OPTICS. - ISSN 0946-2171. - ELETTRONICO. - (2014), pp. 979-986. [10.1007/s00340-014-5917-8]

Availability:

This version is available at: 11583/2528709 since:

Publisher:

Springer

Published

DOI:10.1007/s00340-014-5917-8

Terms of use:

This article is made available under terms and conditions as specified in the corresponding bibliographic description in the repository

Publisher copyright

(Article begins on next page)

High-accuracy coherent optical frequency transfer over a doubled 642-km fiber link

D. Calonico · E. K. Bertacco · C. E. Calosso · C. Clivati ·
G. A. Costanzo · M. Frittelli · A. Godone · A. Mura ·
N. Poli · D. V. Sutyryn · G. Tino · M. E. Zucco · F. Levi

Received: 29 May 2014 / Accepted: 21 August 2014
© Springer-Verlag Berlin Heidelberg 2014

Abstract To significantly improve the frequency references used in radio-astronomy and the precision measurements in atomic physics, we provide frequency dissemination through a 642-km coherent optical fiber link. On the frequency transfer, we obtained a frequency instability of 3×10^{-19} at 1,000 s in terms of Allan deviation on a 5-mHz measurement bandwidth, and an accuracy of 5×10^{-19} . The ultimate link performance has been evaluated by doubling the link to 1,284 km, demonstrating a new characterization technique based on the double round trip on a single fiber. This method is an alternative to previously demonstrated techniques for link characterization. In particular, the use of a single fiber may be beneficial to long hauls realizations in view of a continental fiber network for frequency and time metrology, as it avoids the doubling of the amplifiers, with a subsequent reduction in costs and maintenance. A detailed analysis of the results is presented, regarding the phase noise, the cycle-slips detection and removal and the instability evaluation. The observed noise power spectrum is seldom

found in the literature; hence, the expression of the Allan deviation is theoretically derived and the results confirm the expectations.

1 Introduction

Coherent optical fiber links [1] are the most precise technique to transfer time and frequency signals or to compare remote frequency standards [2–13], as they improve by more than four orders of magnitude the resolution of current satellite techniques [14]. Thus, they are a key technology both for science and metrology, allowing for different outstanding applications.

Presently, optical links are the only viable method for optical clocks comparison. This is a prerequisite for an effective secondary representation of the second in the International System of units [15], as recommended by the Conférence Générale des Poids et Mesures, and for the possible redefinition of the second itself.

Even Cs fountains, presently the best realizations of the SI second, could benefit from optical fiber links as an alternative to satellite techniques [14]. In fact, optical links would reduce by a factor 20 the measuring time needed to compare primary standards at their accuracy level.

Moreover, optical links pave the way for a network of accurate clocks. For instance, in Europe, there are about thirty atomic clocks between optical and fountain frequency standards. This network would establish a unique facility for testing fundamental physics, relativistic geodesy and for improving global navigation satellite systems [16–18].

In addition, optical links could improve the synchronization in very long baseline interferometry (VLBI) antennas and particle accelerators [19–21].

D. Calonico · E. K. Bertacco · C. E. Calosso · C. Clivati (✉) ·
G. A. Costanzo · M. Frittelli · A. Godone · A. Mura ·
M. E. Zucco · F. Levi
Istituto Nazionale di Ricerca Metrologica INRIM, Strada delle
Cacce 91, 10135 Turin, Italy
e-mail: c.clivati@inrim.it

G. A. Costanzo
Politecnico di Torino, Corso Duca degli Abruzzi 24,
10129 Turin, Italy

N. Poli · D. V. Sutyryn · G. Tino
Università di Firenze, LENS and INFN, Via Sansone 1,
Sesto Fiorentino, FI, Italy

Most of these applications require fiber hauls of 1,000s of kilometers, and this is a challenge for performances, installation costs, and link characterization.

This work presents the optical fiber link of 642 km implemented in Italy, named Italian Link for Time and Frequency (LIFT) [22]. LIFT connects the Italian metrological institute (INRIM) to several Italian scientific poles which would largely benefit from improved frequency references. In particular, as shown in the map in Fig. 1, the fiber link provides a reference signal to the Institute for Photonics and Nanotechnologies in Milan, to the Institute for Radio-Astronomy in Medicina (Bologna) and to the University of Florence-European Nonlinear Spectroscopy Laboratory (UNIFI-LENS) in Florence for precision measurements in atomic and molecular physics. LIFT will also connect Italy to the forthcoming European fiber network.

To characterize the ultimate performance of the link in terms of residual phase noise and frequency uncertainty at the far fiber end, we need to compare the frequency of the delivered and of the original signal. Two different techniques have been proposed so far in the literature that are based either on the development two antiparallel optical links on independent fibers [2] or on the looping of the link

using two independent fibers, so that both ends are in the same laboratory [3]. The implementation of one or the other technique strongly depends on technical considerations such as the link phase noise, the attenuation and the available amplifiers.

In our experiment, we looped the link so that the signal goes from INRIM to UNIFI-LENS and then comes back to INRIM, after travelling the link twice, for a total length of 1,284 km in the optical fiber. In fact, this technique enables the characterization of the doubled link and poses an upper limit to the uncertainty contribution of the frequency transfer on a single link.

In this work, we demonstrate that it is not necessary to use two independent fibers for this characterization. This avoids the need of developing a separate twin link for the bare characterization purpose: the number of amplifiers is halved and the reduction of the costs and of the infrastructure complexity may benefit the effective implementation of continental long hauls. Different approaches have been proposed in the literature to analyze the link instability and inaccuracy [3, 4]. We contribute to this discussion, also addressing some relevant issues in the use of the Allan deviation estimator for the observed link phase noise.

Fig. 1 The map of the coherent optical fiber link. View from North to South. *TO* Turin, *MI* Milan, *BO* Bologna, *FI* Florence (elaboration based on GoogleEarth)



2 Experimental setup and results

The infrastructure is based on a dedicated fiber 642 km long, with 171 dB losses compensated by nine bidirectional erbium doped fiber amplifiers (bEDFA). For a 18 dB gain and on a bandwidth of 0.1 nm, these devices exhibit an amplified spontaneous emission (ASE) of -35 dBm at 0.5 nm from the coherent carrier at 1,542.14 nm, of -38 dBm at 1,561.4 nm and of -28 dBm at 1,529.6 nm. This large ASE is filtered on a bandwidth of 0.8 nm by eight telecom optical filters to prevent the amplifiers gain saturation and the onset of auto-oscillations [23]. In a single shelter, the optical filtering did not lead to improved performances and therefore was not employed. Table 1 shows the amplifiers shelters location and the optical loss/gain for each fiber span, and Fig. 2 shows the measured phase noise on the haul between INRIM and some intermediate locations along the backbone. Interestingly, the phase noise shows a broad peak at frequencies between 10 and 20 Hz. A similar behavior has been reported in other published results [4, 9, 24] and has been attributed to building and ground vibrations [4].

The delivered optical radiation is provided by a fiber laser at 1,542.14 nm, frequency-stabilized to an ultrastable Fabry–Perot cavity that reduces the laser linewidth to 30 Hz [25]. To avoid the stability deterioration of the delivered signal due to temperature variations and mechanical stresses of the fiber, the link is phase-stabilized through the Doppler noise cancellation technique [1, 13]. The setup is shown in Fig. 3a. The ultrastable laser L1 is the local oscillator, sent to UNIFI-LENS; few milliwatts of optical power are coupled into the fiber. In the remote

laboratory, a part of the signal is extracted and represents the delivered ultrastable signal, the remainder is reflected back to INRIM by a Faraday mirror (FM), that constantly rotates the reflected beam polarization by 90° as compared to the injected beam polarization. The acousto-optic fixed frequency shifter AOM2, at about 40 MHz, is used to distinguish the reflected signal from undesired backreflections along the fiber that are not frequency-shifted. At INRIM, the round-trip signal is phase-compared to the local laser on photodiode PD1. The pair of FMs placed at the local and remote link end enables to constantly maximize the polarization alignment of the two beatnote arms on PD1, regardless of the fiber birefringence variations [3]. This beatnote contains the information about the noise added by the fiber on the round trip. It is used to stabilize the link with a phase-locked loop (PLL) acting on the acousto-optic modulator AOM1, operating at about 40 MHz.

Usually, the characterization of optical links is pursued by using a couple of fibers in the same bundle, with an independent set of amplifiers [2, 3]. In this work, we demonstrate a characterization technique that uses only one fiber, thus requiring half of the amplifiers. The setup is shown in Fig. 3b. The L1 radiation travels to UNIFI-LENS and is reflected back to INRIM, where it is extracted through the splitter S. A second independent ultrastable fiber laser L2 works as a cleanup oscillator for the incoming signal and is phase locked to it on a bandwidth of about 50 kHz by acting on the acousto-optic modulator AOM3, operating at 79 MHz. The cleanup radiation travels the doubled link in the backward direction, to provide a double-round-trip signal, needed for the 1,284 km link stabilization.

Table 1 The amplifiers placement and the losses/gains for each span

From	To	Length (km)	Loss (dB)	Gain (dB)
1. INRIM	Turin (city)	25	-9	
2. Turin (city)	Santhià	67	-18	19
3. Santhià	Novara	77	-18	16
4. Novara	Lainate	50	-15	13
5. Lainate	Milan	60	-18	20
6. Milan	Piacenza	67	-16	17
7. Piacenza	Reggio Emilia	94	-23	19
8. Reggio Emilia	Bologna	74	-19	16
9. Bologna	Rioveggio	38	-10	17
10. Rioveggio	Florence	72	-18	19
11. Florence	UNIFI-LENS	18	-7	
Total		642	-171	156

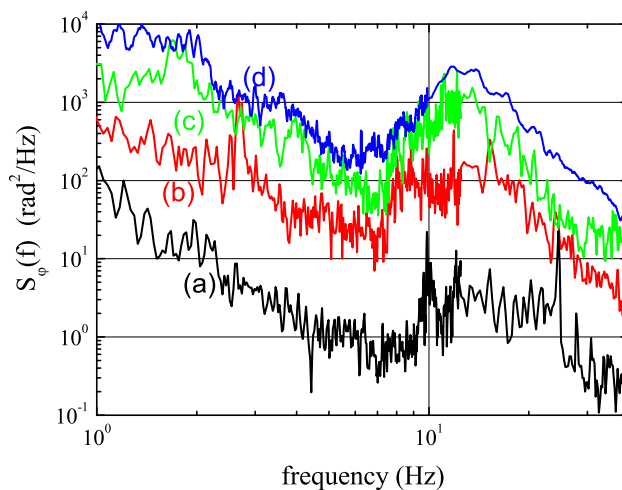


Fig. 2 The measured phase noise of the hauls between INRIM and some relevant places along the backbone. **a**, Black Turin (city), 25 km; **b**, red Novara, 169 km; **c**, green Piacenza, 347 km; **d**, blue Florence, 642 km

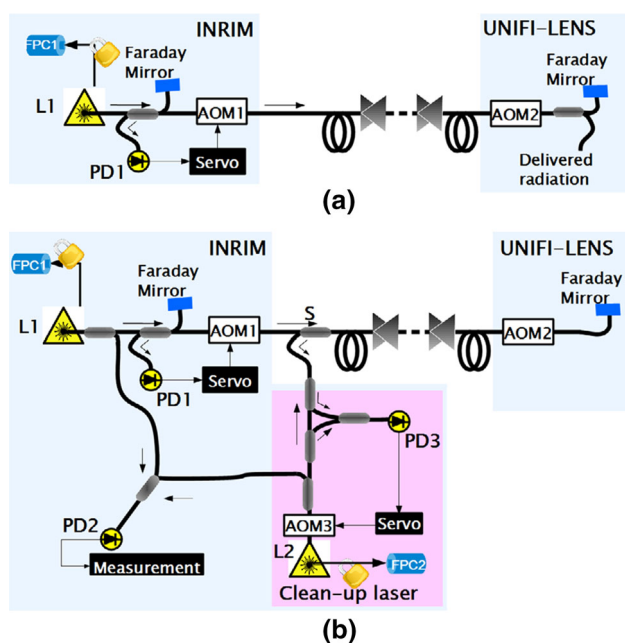


Fig. 3 **a** The setup of the link Turin–Florence. The radiation from laser $L1$ is frequency locked to a Fabry–Pérot cavity (FPC1) and injected in the link. AOM1 and AOM2 are the local and remote acousto-optic modulators, PD1 is the photodiode used to detect the fiber noise. Triangles represent bEDFA. **b** The setup of the doubled link. The laser coming back from Florence is extracted and regenerated through the cleanup laser $L2$. $L2$ is pre-stabilized on a Fabry–Pérot cavity (FPC2) then phase locked to the round-trip signal; AOM3 is the actuator. A part of the radiation from $L2$ is injected in the link toward Florence for the second round trip; the remainder is phase-compared to $L1$ on PD2

The cleanup laser is required due to the relevant wide-band noise added by the optical amplifiers and enables to achieve a signal to noise ratio >24 dB on a bandwidth of 30 kHz on the beatnote detected on PD1, which is the minimum bandwidth required to stabilize the doubled link. Its use was first proposed by [3], where a free-running narrow-linewidth laser diode was directly phase locked to the incoming radiation. In our setup, we pre-stabilized the cleanup laser on a Fabry–Pérot cavity to reduce the phase noise on the beatnote. This is because our optical phase lock relies on analog mixers that have a limited dynamic range as compared to the digital phase-frequency detectors used in previous implementation [3]. The clean up radiation is up-shifted in frequency by 368 MHz with respect to the incoming one; the large frequency separation between the signals in each of the four passes allows a good rejection of the single Rayleigh scattering, which has a bandwidth of few kilohertz, and avoids any crosstalk between the signals. The link performances are analyzed by directly comparing $L2$ – $L1$ on the photodiode PD2. The PD2 beatnote is tracked by a voltage-controlled oscillator, and its phase noise spectrum is shown in Fig. 4, both in the

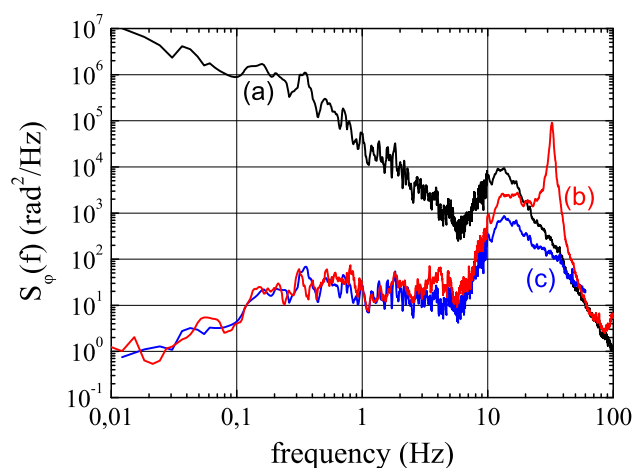


Fig. 4 Phase noise spectrum of the free-running (black line, **a**) and compensated (red line, **b**) 1,284 km optical fiber link, and the residual phase noise expected from theory (blue line, **c**)

free-running (black line) and in the Doppler-compensated link configuration (red line). Because the doubled link delay is $\tau = nL/c = 6.4$ ms, with $n = 1.468$ the refractive index of the fiber, c the speed of light in vacuum and $L = 1,284$ km, the loop bandwidth is about 39 Hz. The noise of the compensated link achieves the fundamental limit (blue line) set by the round-trip delay [13] and demonstrates that uncontrolled effects are not observed at this level. We calculated the round-trip delay limit following the approach described in [13], where it is demonstrated that $S_\phi(f) = a(2\pi f\tau)^2 S_{\text{fiber}}(f)$, being $S_{\text{fiber}}(f)$ the noise of the fiber haul.

We calculated $a = 1/4$ rather than $a = 1/3$, since in our case a single fiber is used instead of two independent ones; a detailed derivation is given in the “Appendix”.

In order to optimize the link performances, the gain of each amplifier is tuned to notably reduce the double backreflections along the fiber, which would otherwise dominate the phase noise of the delivered signal.

Another detrimental effect is the loss of phase coherence (cycle slips) [26] on the PLLs that affects both the instability and the inaccuracy of the link. The cycle-slips rate mainly depends on the signal to noise ratio of the beatnotes. In our setup, the two beatnotes are detected with a variable signal to noise ratio of 24–31 dB on a 30-kHz bandwidth, due to long-term variations of the optical power; the polarization is adjusted every few hours to maximize the beatnote power on PD2, and in these optimized conditions, the cycle slips are a few per hour and the link can operate for several hours without unlocks.

The phase of the beatnote on PD2 is measured with a dead-time-free digital phase recorder [27] at the sampling rate of 1 ms, equivalent to a 500-Hz bandwidth filter. The cycle slips are barely visible on the phase data even when

low-pass filtered at 1 Hz bandwidth, as shown in Fig. 5 (red line); however, if we filter the data on a bandwidth of 0.05 Hz (black line) their detection is quite easy.

Particular care is devoted to the filtering process: instead of applying a simple average to the raw data, that acts like a first order low-pass filter with cut-off frequency at half the reciprocal of the averaging time, we implemented a digital finite impulse response (FIR) filter [28], with an out-of-bandwidth attenuation >70 dB between 10 and 100 Hz. The sharper filtering allows a factor 2 of improvement in the stability for the same equivalent bandwidth. This is related to the peculiar phase noise power spectra which are often found in optical links, as will be discussed later on in the text.

We realign the phase by subtracting an integer number of 0.5 cycles, i.e. the minimum slip amplitude. Finally, the phase data are further filtered on a 5-mHz bandwidth (smooth blue line in Fig. 5), decimated according to the Nyquist theorem and differentiated to obtain the instantaneous frequency.

The ultimate frequency instability of the optical link was evaluated using the Allan deviation [29] associated to a strong data filtering, as an alternative to the use of a A -type counter and the modified Allan deviation.

In the literature, its expression is derived from the phase noise spectrum only in the cases where it is modeled by the relation [31]:

$$S_\varphi(f) = \sum_{i=-4}^0 b_i f^i.$$

However, our measurements show a phase noise spectrum of the kind $S_\varphi(f) = b_1 f$, as can be seen in Fig. 4. This noise behavior has already been reported in optical fiber links [4] and depends on the peculiar transfer function of the system, affected by the fiber delay [13]. It is interesting to stress that in this case the carrier does not exist and the radio frequency power spectrum is not defined when a single pole filter limits the phase noise spectral density. This may be demonstrated following the approach reported in [30]. In all physical systems, a natural low-pass filter always exists, thus preventing from the high-frequency noise divergence; still, a proper attenuation of the high-frequency noise must be guaranteed to eliminate any possible sensitivity to the filtering process, as it has been previously noted.

Recently, an expression of the modified Allan deviation for this kind of noise has been published [4], but an analytical expression of the Allan deviation has not been reported yet. We calculate it using the definition

$$\sigma_y^2(t_a) = \int_0^{f_h} S_y(f) |H_A(f)|^2 df, \quad (1)$$

where $S_y(f) = h_3 f^3$ is the relative frequency spectral density, with $h_3 = b_1/v_0^2$ and v_0 the carrier frequency [31]. An

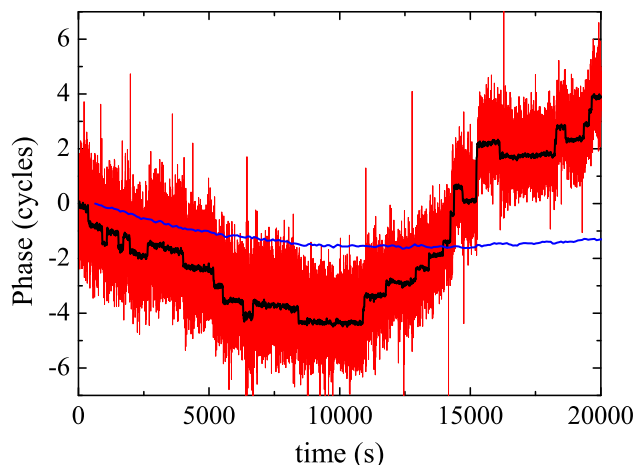


Fig. 5 The phase of the optical carrier as measured on the photodiode PD2 after travelling the doubled link, filtered on a bandwidth of 1 Hz (red line) and 0.05 Hz (black line). Data after the removal of the cycle slips are also shown, on a bandwidth of 5 mHz (blue line)

infinitely-sharp low-pass filter is introduced to avoid the noise divergence at high frequency, f_h is its cut-off frequency, t_a is the averaging time and $|H_A(f)|^2 = 2 \frac{\sin^4(\pi f t_a)}{(\pi f t_a)^2}$ is the squared modulus of the Allan variance transfer function [31]. For $t_a \gg 1/(2\pi f_h)$ the integration leads to:

$$\sigma_y^2(t_a) = \frac{3h_3 f_h^2}{8\pi^2} \frac{1}{t_a^2}. \quad (2)$$

During the link operation, we measured an Allan deviation of $\sigma_y(t_a) = 8 \times 10^{-13}/t_a$ on a 100-Hz measurement bandwidth and of $\sigma_y(t_a) = 8 \times 10^{-14}/t_a$ on a 10-Hz measurement bandwidth. This is in agreement with the prediction of Eq. (2) for the phase noise power spectrum observed in Fig. 4.

Figure 6 shows the Allan deviation of the free-running and compensated optical link on a 1-Hz measurement bandwidth, together with the stability of the compensated link on a 5-mHz bandwidth. The Allan deviation on a 5-mHz bandwidth was obtained after the phase realignment; on the contrary, the data at 1 Hz measurement bandwidth could not be efficiently realigned due to the large noise. Hence, the Allan deviation on this measurement bandwidth was evaluated from a cycles-slips-free region of the data sample shown in Fig. 5.

The link achieves a short-term instability of 1×10^{-14} at 1 s in a 1-Hz bandwidth and an ultimate frequency resolution of 3×10^{-19} in a 5-mHz bandwidth.

The fractional deviation of the transferred frequency from the original one is calculated from the arithmetic mean of the frequency data after the cycles-slips realignment. From measurements repeated in different days, we observed a non-constant frequency offset at the level of

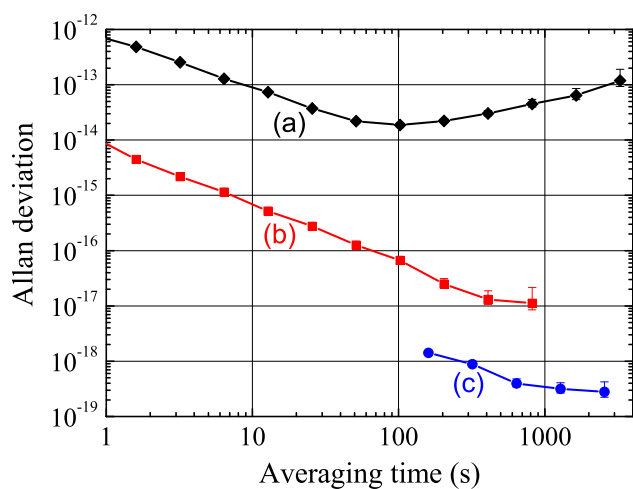


Fig. 6 The frequency instability, expressed as the Allan deviation, of the 1,284-km optical link in free-running (a, black) and compensated (b, red) operation with 1 Hz measurement bandwidth, and the Allan deviation of the compensated link with 5 mHz measurement bandwidth (c, blue). Data have been decimated according to the Nyquist theorem

5×10^{-19} . This has been attributed to long-term phase drifts of the optical signal caused by temperature variations on the short interferometer fibers. These fibers cannot be completely stabilized by the loop, as they are not travelled in a double pass. A long-term phase variation of about one cycle over few hours is observed also in Fig. 5. The same behavior is observed replacing the 642-km fiber with an optical attenuator and is not attributed to the optical link. In spite of this, the present frequency dissemination accuracy is beyond the most challenging requirements of any application and exceeds the world's best oscillators [32, 33].

3 Conclusions

This work describes the realization and characterization of a coherent optical fiber link for frequency transfer over a 642 km haul. The characterization is pursued by doubling the link length to 1,284 km, so that both ends are in the same laboratory. This facility allows a detailed analysis of the link phase noise and of the cycle-slips detection and removal.

The loop has been established using a single fiber; the expected delay-unsuppressed noise is only slightly affected with respect to the value calculated for independent fibers [13]. We avoided the setting-up of a second link; this could be helpful in view of long fiber hauls, as the number of optical amplifiers is considerably reduced. The doubled link is a useful tool to identify the

parameters for an optimal and cycles-slips free operation, such as the signal to noise ratio on the beatnotes, the gain of the amplifiers and the optical power level in the link; this proves to be especially useful if the remote link end is not equipped with ultrastable lasers and phase noise analysis instruments. Other techniques for the real-time link monitoring have been proposed in the literature [2].

In the data analysis, we addressed the use of the Allan deviation associated to narrow-bandwidth filtering, which allows a resolution equivalent to that obtained using other statistical estimators [4].

On the doubled link, we obtain a short-term Allan deviation of 1×10^{-14} at 1 s on the bandwidth of 1 Hz and an ultimate accuracy on the frequency transfer of 5×10^{-19} at 1,000 s integration time. This is also an upper limit for the real dissemination over the 642-km link.

The present infrastructure is now being used for the delivery of a high-accuracy frequency reference at LENS and will benefit the atomic physics experiments which are performed in this laboratory. The haul will soon be upgraded to perform the frequency dissemination to the Institute of Photonics and Nanotechnologies in Milan and to the Medicina Radio-Telescopes, near Bologna, for the VLBI antennas synchronization. Extraction topologies such as those reported in [34–36] are being considered as well as alternative techniques for the remote frequency comparisons [37], and Raman optical amplification [38] is being investigated as an alternative to the present architecture based on BEDFA.

Acknowledgments We thank Gesine Grosche and Paul-Eric Pottie for technical help, Giorgio Santarelli for useful discussions, and the GARR Consortium for technical help with the fibers. This work was supported by: the Italian Ministry of Research MIUR under the Progetti Premiali programme and the PRIN09-2009ZJJBLX project; the European Metrology Research Programme (EMRP) under SIB-02 NEAT-FT. The EMRP is jointly funded by the EMRP participating countries within EURAMET and the European Union.

Appendix

This appendix demonstrates the formula for the delay-unsuppressed noise on a link with both ends in the same laboratory, and where the same fiber is used to loop the link, instead of two independent fibers. An approach similar to the one used in [13] has been followed.

Let us write the expression for the round-trip optical phase $\varphi_{rt}(t)$ and for the forward signal optical phase $\varphi_{fw}(t)$, as a function of the fiber noise $\delta\varphi(z, t)dz$ of an infinitesimal fiber segment dz at time t and position z along the fiber and as a function of the phase correction needed for the link stabilization $\varphi_c(t)$.

$$\begin{aligned}
 \varphi_{\text{rt}}(t) &= \varphi_{\text{c}}(t - 2\tau) + \varphi_{\text{c}}(t) \\
 &+ \int_0^{L/2} \left(\delta\varphi\left(z, t - 2\tau + n\frac{z}{c}\right) + \delta\varphi\left(z, t - \tau - n\frac{z}{c}\right) \right. \\
 &+ \left. \delta\varphi\left(z, t - \tau + n\frac{z}{c}\right) + \delta\varphi\left(z, t - n\frac{z}{c}\right) \right) dz \\
 \varphi_{\text{fw}}(t) &= \varphi_{\text{c}}(t - \tau) \\
 &+ \int_0^{L/2} \left(\delta\varphi\left(z, t - \tau + n\frac{z}{c}\right) + \delta\varphi\left(z, t - n\frac{z}{c}\right) \right) dz
 \end{aligned} \tag{3}$$

where L is the loop length, in our case $L = 1,284$ km, and $\tau = nL/c$ is the link delay. For the sake of clarity, we integrate the length only between 0 and $L/2$, as the two fiber halves are indeed the same fiber travelled in opposite directions.

Let us now assume that the fiber perturbations evolve linearly with time; this is justified for perturbations which act on timescales much longer than τ , as in the case of interest in this context. Within this approximation, Eq. 3 is simplified into

$$\begin{aligned}
 \varphi_{\text{rt}}(t) &= 2\varphi_{\text{c}}(t - \tau) + \int_0^{L/2} 4\delta\varphi(z, t - \tau) dz \\
 \varphi_{\text{fw}}(t) &= \varphi_{\text{c}}(t - \tau) + \int_0^{L/2} 2\delta\varphi\left(z, t - \frac{\tau}{2}\right) dz
 \end{aligned} \tag{4}$$

Now, considering that in the closed feedback loop configuration $\varphi_{\text{rt}}(t, z) = 0$, Eq. 4 is rewritten as

$$\begin{aligned}
 \varphi_{\text{fw}}(t) &= 2 \int_0^{L/2} \left(\delta\varphi\left(z, t - \frac{\tau}{2}\right) - \delta\varphi(z, t - \tau) \right) dz \\
 &= 2 \int_0^{L/2} \frac{\tau}{2} \frac{d}{dt} \delta\varphi(z, t - \tau) dz
 \end{aligned} \tag{5}$$

In the last equation, the evolution of the fiber noise is expressed as a function of its time derivative. For the fundamental theorem of the signal analysis [39], the noise power spectrum of the output of a linear and time-invariant system can be written in terms of the noise of the input; in our case, this theorem can be applied to each fiber segment separately, i.e.:

$$S_{\varphi}(z, f) = |H(z, f)|^2 S_{\text{fiber}}(z, f), \tag{6}$$

where $S_{\varphi}(z, f)$ is the contribution of a fiber segment with length dz to the compensated forward signal phase noise, $H(z, f) = \mathcal{F}\left(\tau \frac{d}{dt}\right) = 2\pi i f \tau$ and $S_{\text{fiber}}(z, f)$ is the phase noise power spectrum of each fiber segment. Assuming that the contributions of each fiber segment are independent, we can perform the integration and end up with the stated result that

$$S_{\varphi}(f) = \frac{1}{4} (2\pi f \tau)^2 S_{\text{fiber}}(f), \tag{7}$$

where $S_{\text{fiber}}(f)$ is the phase noise of the 1,284-km-long link, and it has been used in the relation

$$S_{\text{fiber}}(f) = 4 \int_0^{L/2} |\delta\varphi(z, t)|^2 dz.$$

References

1. L.-S. Ma, P. Jungner, J. Ye, J.L. Hall, *Opt. Lett.* **19**, 1777 (1994)
2. K. Predehl, G. Grosche, S.M.F. Raupach, S. Droste, O. Terra, J. Alnis, T. Legero, T.W. Hänsch, Th Udem, R. Holzwarth, H. Schnatz, *Science* **336**, 441 (2012)
3. O. Lopez, A. Haboucha, B. Chanteau, C. Chardonnet, A. Amy-Klein, G. Santarelli, *Opt. Express* **20**, 23518 (2012)
4. S. Droste, F. Ozimek, Th Udem, K. Predehl, T.W. Hansch, H. Schnatz, G. Grosche, R. Holzwarth, *Phys. Rev. Lett.* **111**, 110801 (2013)
5. O. Lopez, A. Kanj, P. Pottie, D. Rovera, J. Achkar, C. Chardonnet, A. Amy-Klein, G. Santarelli, *Appl. Phys. B* **110**, 3 (2013)
6. L. Sliwczyski, P. Krehlik, A. Czubla, L. Buczek, M. Lipiski, *Metrologia* **50**, 133 (2013)
7. B. Wang, C. Gao, W.L. Chen, J. Miao, X. Zhu, Y. Bai, J.W. Zhang, Y.Y. Feng, T.C. Li, L.J. Wang, *Sci. Rep.* **2**, 556 (2012)
8. G. Marra, R. Slavik, H.S. Margolis, S.N. Lea, P. Petropoulos, D.J. Richardson, P. Gill, *Opt. Lett.* **36**, 511 (2011)
9. M. Fujieda, M. Kumagai, S. Nagano, A. Yamaguchi, H. Hachisu, T. Ido, *Opt. Express* **19**, 16498 (2011)
10. S.-C. Ebenhag, P.O. Hedekvist, P. Jarlemark, R. Emardson, K. Jaldehag, C. Rieck, P. Löthberg, *IEEE Trans. Instrum. Meas.* **59**, 1918 (2010)
11. F.-L. Hong, M. Musha, M. Takamoto, H. Inaba, S. Yanagimachi, A. Takamizawa, K. Watabe, T. Ikegami, M. Imae, Y. Fujii, M. Amemiya, K. Nakagawa, K. Ueda, H. Katori, *Opt. Lett.* **34**, 692 (2009)
12. J. Vojtech, V. Smotlacha, P. Skoda, A. Kuna, M. Hula, S. Sima, in *Proceedings of the SPIE 8516. Remote Sensing System Engineering IV*, San Diego, CA, 2012, p. 85160H
13. P.A. Williams, W.C. Swann, N.R. Newbury, *J. Opt. Soc. Am. B* **25**, 1284 (2008)
14. A. Bauch, J. Achkar, S. Bize, D. Calonico, R. Dach, R. Hlavac, L. Lorini, T. Parker, G. Petit, D. Piester, K. Szymaniec, P. Urich, *Metrologia* **43**, 109 (2006)
15. Burea international des poids et mesures, in *Comptes rendus de la 23^e réunion de la Conférence générale des poids et mesures*, 12–16 Nov 2007, BIPM, Sèvres, France, 2010, p. 431
16. C.W. Chou, D.B. Hume, T. Rosenband, D.J. Wineland, *Science* **329**, 1630 (2010)
17. J. Müller, M. Soffel, S.A. Klioner, *J. Geod.* **82**, 133 (2008)
18. G. Cerretto, N. Guyennon, I. Sesia, P. Tavella, F. Gonzalez, J. Hahn, V. Fernandez, A. Mozo, in *Proceedings of the European Frequency and Time Forum*, Toulouse, France, 2008
19. Y. He, B.J. Orr, K.G.H. Baldwin, M.J. Wouters, A.N. Luiten, G. Aben, R.B. Warrington, *Opt. Express* **21**, 18754 (2013)
20. J.F. Cliche, B. Shillue, *IEEE Control Syst. Mag.* **26**, 19 (2006)
21. J. Kim, J.A. Cox, J. Chen, F.X. Kärtner, *Nat. Photonics* **2**, 733 (2008)
22. F. Levi, R. Ambrosini, D. Calonico, C.E. Calosso, C. Clivati, G.A. Costanzo, P. De Natale, D. Mazzotti, M. Frittelli, G. Galzerano, A. Mura, D. Sutyryn, G.M. Tino, M.E. Zucco, N. Poli, in *Proceedings of the Joint UFFC, EFTF and PFM Symposium*, 2013, pp. 477–480

23. C. Delisle, J. Conradi, J. Lightwave Technol. **15**, 749–757 (1997)
24. O. Terra, G. Grosche, K. Predehl, R. Holzwarth, T. Legero, U. Sterr, B. Lipphardt, H. Schnatz, Appl. Phys. B **97**, 541 (2009)
25. C. Clivati, D. Calonico, C.E. Calosso, G.A. Costanzo, F. Levi, A. Mura, A. Godone, IEEE Trans. Ultrason. Ferroelectr. Freq. Control. **58**, 2582 (2011)
26. Th Udem, J. Reichert, T.W. Hänsch, M. Kourogi, Opt. Lett. **23**, 1387 (1998)
27. G. Kramer, W. Klische, in *Proceedings of the 2001 IEEE International Frequency Control Symposium and PDA Exhibition*, Seattle, WA, 2001, p. 144
28. S.K. Mitra, *Digital Signal Processing* (McGraw-Hill, New York, 2006)
29. D. Allan, in *Proceedings of the IEEE* 54, 1966, p. 221
30. A. Godone, S. Micalizio, F. Levi, Metrologia **45**, 313 (2008)
31. E. Rubiola, *Phase Noise and Frequency Stability in Oscillators* (Cambridge University Press, Cambridge, 2009)
32. B.J. Bloom, T.L. Nicholson, J.R. Williams, S.L. Campbell, M. Bishof, X. Zhang, W. Zhang, S.L. Bromley, J. Ye, Nature **506**, 7175 (2014)
33. I. Ushijima, M. Takamoto, M. Das, T. Ohkubo, H. Katori, <http://arxiv.org/abs/1405.4071>
34. A. Bercy, S. Guellati-Khelifa, F. Stefani, G. Santarelli, C. Chardonnet, P.-E. Pottie, O. Lopez, A. Amy-Klein, J. Opt. Am. Soc. B **31**, 698 (2014)
35. S.W. Schediwy, D. Gozzard, K.G.H. Baldwin, B.J. Orr, R.B. Warrington, G. Aben, A.N. Luiten, Opt. Lett. **38**, 2893 (2013)
36. G. Grosche, Opt. Lett. **39**, 2545 (2014)
37. C.E. Calosso, E. Bertacco, D. Calonico, C. Clivati, G.A. Costanzo, M. Frittelli, F. Levi, A. Mura, A. Godone, Opt. Lett. **39**, 11771180 (2014)
38. C. Clivati, G. Bolognini, D. Calonico, S. Faralli, F. Levi, A. Mura, N. Poli, Photonics Technol. Lett. **25**, 1711 (2013)
39. A. Papoulis, in *Probability, Random Variables, and Stochastic Processes*. International Student Edition (McGraw Hill, Kogakusha, 1965), p. 347